NISTIR 6588

FIFTEENTH MEETING OF THE UJNR PANEL ON FIRE RESEARCH AND SAFETY MARCH 1-7, 2000

VOLUME 2

Sheilda L. Bryner, Editor

National Institute of Standards and Technology
Technology Administration, U.S. Department of Commerce

NISTIR 6588

FIFTEENTH MEETING OF THE UJNR PANEL ON FIRE RESEARCH AND SAFETY MARCH 1-7, 2000

VOLUME 2

Sheilda L. Bryner, Editor

November 2000

U. S. Department of Commerce
Norman Y. Mineta, Secretary
Technology Administration
Dr. Cheryl L. Shavers, Under Secretary of Commerce for Technology
National Institute of Standards and Technology
Raymond G. Kammer, Director

FIRE SPREAD BY BRAND SPOTTING

Patrick J. Pagni and John P. Woycheese
Mechanical Engineering Department
University of California
Berkeley, CA 94720-1740 USA

Introduction

Burning brands, lofted above large fires and propagated by the prevailing winds, can cause spot ignitions far from the flame front. These distant and unexpected fires are an important mechanism for fire spread in post-earthquake and urban/wildland intermix fires. The 20 October Oakland Hills Fire quickly overwhelmed fire fighting efforts, in part due to brand propagation and spotting hundreds of meters ahead of the fire front [1]. Although spotting has received considerable attention from the forest fire community [2-7], little research quantifies brand propagation from structures or rubble piles.

Fire spread by brand spotting consists of three elements: lofting, propagation, and deposition with fire initiation. Previous research has either de-coupled the lofting and propagation phases[8-12] or added simple linear combinations of plume and ambient winds[5, 6, 8] due to the complex nature of the velocity field around and above large fires. New models are now available that utilize Large Eddy Simulation (LES) to enable calculation of terrain, ambient wind, and atmospheric effects on large fire plumes [13-15].

LES models require a number of brand characteristics to calculate spotting location distances accurately. The heterogeneous combustion of brands, coupled with size and shape histories, present considerable research challenges. Initial brand conditions such as size, shape, and material properties are assumed [2, 5, 8-12]. The gravitational and aerodynamic forces can be approximated analytically. To describe these forces, the brand shape, size, mass, and drag and lift coefficients are required as functions of time. The forces to which the brand is subjected are illustrated in Fig. 1, which can be expanded to three dimensions. Drag acts in the direction of relative velocity, **W**, which is the difference between the brand velocity and that of the surrounding velocity field. Lift acts perpendicular to drag, and the force due to gravity pulls the disk downward. Note that non-rotating spherical and cylindrical brands, which have axes of symmetry perpendicular to the relative velocity field in their most stable orientation, will not have lift; the lift and drag forces for disks are dependent on the angle of attack, α [16].

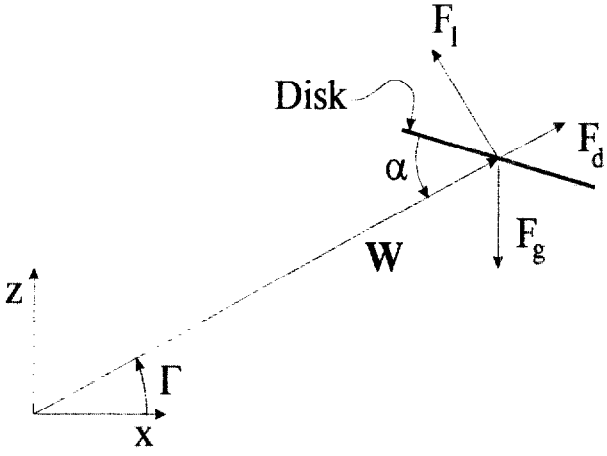

Figure 1: Summary of the forces acting on a combusting brand in an irrotational relative velocity field, W

Prior to lofting and propagation, brands are usually assumed to be well-formed; i.e., combustion will have smoothed corners and other sharp edges, so that lofted brands will primarily consist of spheres, cylinders , and disks. Previous research and experiments have concentrated on the former two shapes [2-11, 17-21]; from Fig. 2, however, it can be seen that more massive brands can be lofted as disks than as spheres or cylinders. The small drag coefficient and large mass-to-cross-sectional-area ratio severely limits the propagation range of spheres relative to the other shapes; likewise, the weight-to-drag ratio of cylinders falls short of that for disks. Therefore, this paper focuses on disks and the experimental determination of their combustion histories.

There are two stages to brand combustion: flaming combustion, and surface, or glowing, combustion. Not all wood types utilize both combustion phenomena. In the flaming mode, pyrolysis appears to cause significant mass loss with little change in the brand dimension. After this initial period, the pyrolysis rate becomes restricted by char formation. The brand size then decreases slowly as char is consumed by surface combustion. Glowing

combustion provides mass and size changes until combustion can no longer be sustained or until the brand is completely consumed.

Experimental Procedure

The primary goal of this work is to provide experimental brand size and shape data as a function of time for comparison with a variety of combustion models [12]. There have been several experiments to provide the mass and/or terminal velocity for brands, but there is a lack of data for size and shape change. These experiments are being conducted with two methodologies: videographic and gravimetric.

Table 1: Experiments to Self-Extinguishment, by Length-to-Diameter Ratio

Wood Type	50 mm diameter			25 mm diameter		
	1 m/s	2 m/s	4 m/s	1 m/s	2 m/s	4 m/s
Oak	1:3, 1:9	1:3, 1:9	1:3, 1:9	1:3	1:3	1:3
Fir	**1:3**, 1:9	**1:3**, 1:9	1:3, 1:9	**1:3**	**1:3**	1:3
Cedar (WRC)				**1:3**	**1:3**	1:3
Balsa	1:3, 1:9	1:3, 1:9	1:3, 1:9	**1:3**	**1:3**	1:3
Dense Balsa	1:3	1:3	1:3			

In the videographic experiments, data for brand size and shape histories is being developed to provide empirical data for the confirmation of combustion models. Data has been gathered at constant velocities with $\alpha = 90°$ on burning brands with diameters of 25 and 50 mm, the range expected for the majority of plume-born brands. Video journals of the brands, taken from two perpendicular views, are used to obtain size changes as functions of time. The videos also record the transitions from flaming to glowing combustion and from full to single-sided combustion. Experiments are being conducted for a range of wood types, brand sizes, and relative velocities – a representative sample is shown in Table 1. All of these data are for end-grain disks. Additional experiments have been performed on transverse-grain disks, with disappointing repeatability. The chosen wood species provide a full range of physical charateristics, including density, thermal inertia, and void space. Figure 3 shows the terminal velocities for several shapes and wood species. Previous analyses have shown that the relative velocity is frequently the terminal velocity. The densities for the experiments conducted are indicated by the vertical dashed lines.

A set of gravimetric experiments is being conducted to determine brand mass, shape, and size as functions of time for a variety of wood types at various wind tunnel speeds. Disk brands are mounted in the wind tunnel and allowed to burn for a set period of time, after which the brand is removed and immerse in CO_2. The final brand size, shape, and weight is compared to initial values and is used to determine the mass history, and to provide more complete data for size and shape histories, for a number of size, velocity, and wood combinations.

Results

Figure 4 provides a side-by-side comparison of two similar experiments conducted on different wood types: fir and cedar. Both experiments were conducted on samples that were 25mm in diameter and 8mm thick (length-to-diameter ratio of 1:3) in a velocity field of 1.8 m/s. The douglas fir sample extinguished approximately 90 sconds after insertion in the wind tunnel, and retained nearly half of its initial mass; the western red cedar sample burned to completion after 210 seconds. These samples illustrate the two paths that different wood samples followed. The more dense samples of oak and douglas fir flame for a longer time, but, in general, do not transition to surface combustion. Complete combustion rarely occurs without significant, persistent surface combustion on the upwind face of the brand. As a result, these samples self-extinguished before a large fraction of their initial mass had combusted. The side and wake flames visible after 20 seconds have elapsed cause the sample to form a truncated cone. At lower speeds, the remaining sample is completely charred, with cupping at the back and bowing at the font. At higher speeds, more than half of the sample is either slightly discolored or virgin wood underneath a thin film of char; at speeds above 4 m/s, the combusion period is too short to cause shape change.

Wood with lower density, such as cedar and balsa, transition from flaming to surface combustion, with the flaming combustion ending relatively early in the brand lifetime. In most cases, the surface combustion starts around the front edge of the brand, and grows to include the entire face. Before the flaming ends, surface combustion commences on the back edge and the brand forms a glowing ellipsoid, as seen in Fig. 4. Unlike flaming combustion, glowing is most active on the face of the sample; the front edges and face combust at a higher rate than the rest of the sample, and the brand forms a truncated hemisphere – with flat edge to back – later in its liftime. Nearly all of the low-density samples, at all tested speeds, burned to completion.

To develop a mass history for a certain wood type, size, and relative velocity, samples are removed from the wind tunnel and extinguished using CO_2. Once extinguished, the samples are weighed and measured. To preserve the specimens for detailed analysis, they are not reignited. Fresh samples are introduced to the same wind tunnel conditions and extracted at later times. A representative mass history for douglas fir is given in Fig. 5. Some of the samples are extinguished immediately after ignition to determine the mass lost during the ignition process; this amounted to 3-4% of the dry mass for fir. Allowing some samples to burn to completion provides the time to self-extinguishment. Other samples are extinguished after a fraction of the average self-extinguishment time to determine the average mass, shape, and size history during combustion. Similar experiments will be conducted for balsa and western red cedar as indicated by the bold entries in Table 1.

The transition time from flaming to surface combustion is illustrated in Fig. 6 for different wood types as a function of relative velocity, while the time to self-extinguishment, or brand extinction time, is shown in Fig. 7. The time of transition from flaming to surface combustion (or immediate extinction) decreases as the relative velocity increases for all wood types. It also appears to be a function of density or thermal inertia, with the flaming time increasing with increasing density. For douglas fir, the extinction time is closely linked to flaming combustion. Typically, fir does not transit to surface combustion when the flames extinguish. The increase in extinction time at 2.4 m/s is the result of an anomaly where an area less than five mm^2 continued to burn for tens of seconds after the flames ceased. At 1 and 4 m/s, oak burned in much the same fashion; at 2 m/s, however, a small ring of surface combustion formed around the back edge of the brand, due to favorable recirculation velocities downwind of the brand, increased the combustion time by 50%. The mass loss and size change during this latter combustion period was small. Both the flaming and the extinction times for both varieties of balsa decreased with increasing velocity. Glowing combustion represents a significant fraction of the total brand lifetime. These samples burned to completion. The mass fraction at extinction, or residual mass, for 50-mm-diameter, 16-mm-thick oak and fir disks is shown in Fig. 8 as a function of relative velocity. The increase in residual mass with increasing velocity as is expected.

Conclusions

Of the species examined here, the lighter wood species, western red cedar and balsa, appear to burn to completion via glowing surface combustion. The denser wood species, oak and douglas fir, self-extinguish once flaming ceases with considerable residual mass. There is also a strong dependence on wood grain orientation. All of the data in these figures were obtained with an end grain facing the relative velocity vector. Preliminary experiments with transverse grain facing the relative velocity vector show that these also tend to burn primarily where the end grain is exposed; i.e., at the edge. It is possible that the brands with the longest lifetimes will be those with relatively little shape, size, and mass change that are glowing only on a small portion of the disk edge. This seems to further indite cedar shakes and shngles, which start with an aerodynamically advantageous shape, burn well via surface glowing after flaming ceases, and have grain orientations that encourage edge burning.

This is a work in progress. Approximately one-third of the experiments in Table 1 remain to be done. Wood is a difficult experimental material. Perhaps a better approach would have been to start with these experiments, rather than with analytical studies [10-12]. Different species and grain orientations need further exploration. Aerodynamic effects such as tumbling, i.e., varying angle of attach, and varying velocity require study. Future burning models for various brand shapes developed from these experiments may be inserted as Lagrangian particles into LES fire plume models [13-15], which describe the interaction of the flow field from large fires with complex terrain and ambient winds, to develop probabilistic distributions of spot fires given fire, fuel, geographic, and atmospheric parameters.

Acknowledgements

We are grateful for the continuing financial support provided by the Building and Fire Research Laboratory of the National Institute of Standards and Technology, U.S.D.O.C., under Grant No. 60NANB80D0094, and by a student grant from the Educational and Scientific Foundation of the Society of Fire Protection Engineers.

References

1. Pagni, P.J., "Causes of the 20th October 1991 Oakland Hills Conflagration," *Fire Safety Journal*, **21**:4, 331-340, 1993.
2. Muraszew, A., "Firebrand Phenomena," *Aerospace Report No. ATR – 74 (8165 –01) –1*, The Aerospace Corporation, El Segundo, 1974.
3. Muraszew, A., Fedele, J.B., and Kuby, W.C., "Firebrand Investigation," *Aerospace Report ATR-75 (7470) –1*, The Aerospace Corp., El Segundo, CA, 1975.
4. Muraszew, A., and Fedele, J.B., "Statistical Model for Spot Fire Hazard," *Aerospace Report No. ATR – 77 (7588) –1*, The Aerospace Corporation, El Segundo, 1976.
5. Albini, F.A., "Spot Fire Distance From Burning Trees: A Predictive Model," *General Technical Report No. INT – 56*, USDA Forest Service Intermountain Forest and Range Experiment Station, Ogden, UT, 1979.
6. Albini, F.A., "Potential Spotting Distance from Wind-Driven Surface Fires," *USDA Forest Service Research Paper INT-309*, USDA, 1983.
7. Albini, F.A., "Transport of Firebrands by Line Thermals," *Combustion Science and Technology*, **32**, 277-288, 1983.
8. Tarifa, C.S., del Notario, P.P., and Moreno, F.G., "On the Flight Paths and Lifetimes of Burning Particles of Wood," *Tenth Symposium (International) on Combustion*, 1021-1037, The Combustion Institute, 1965.
9. Tarifa, C.S., del Notario, P.P., Moreno, F.G., and Vill, A.R., "Transport and Combustion of Firebrands," *Final Report of Grants FG-SP-114 and FG-SP-146*, Vol. 2, USDA, Madrid, 1967.
10. Woycheese, J.P., Pagni, P.J., and Liepmann, D., " Brand Propagation From Large-Scale Fires," *Journal of Fire Protection Engineering*, 1998, in review.
11. Woycheese, J.P., Pagni, P.J., and Liepmann, D., "Brand Lofting Above Large-Scale Fires," *Proceedings of the Second International Conference on Fire Research and Engineering*, 137-150, Society of Fire Protection Engineers, Washington, 1998.
12. Woycheese, J.P., and Pagni, P.J., "Combustion Models for Wooden Brands," *Proceedings of the Third International Conference on Fire Research and Engineering*, 53-71, Society of Fire Protection Engineers, Washington, 1999.
13. McGrattan, K.B., Ferek, R.J., and Uthe, E.E., "Smoke Plume Trajectory from In Situ Burning of Crude Oil – Field Experiments," *Proceedings of the First International Conference on Fire Research and Engineering*, ed. D. Peter Lund, 47-52, Society of Fire Protection Engineers, Orlando, FL, 1995.
14. McGrattan, K.B., Rehm, R.G., Tang, H.C., and Baum, H.R., "A Boussinesq Algorithm for Buoyant Convection in Polygonal Domains," *NISTIR 4831*, National Institute of Standards and Technology, Gaithersburg, MD, 1992.
15. McGrattan, K.B., Baum, H.R., Walton, W.D., and Trelles, J., "Smoke Plume Trajectory from In Situ Burning of Crude Oil in Alaska – Field Experiments and Modeling of Complex Terrain," *NISTIR 5958*, National Institute of Standards and Technology, Gaithersburg, MD, 1997.
16. Hoerner, S.F., *Fluid-Dynamic Drag*, Published by author, 1958.
17. Lee, S.-L., and Hellman, J.M., "Firebrand Trajectory Study Using an Empirical Velocity-Dependent Burning Law," *Combustion and Flame*, **15**:3, 265-274, 1970.
18. Lee, S.-L., and Hellman, J.M., "Study of Firebrand Trajectories in a Turbulent Swirling Natural Convection Plume," *Combustion and Flame*, **13**:6, 645-655, 1989.
19. Phillips, A.M., and Becker, H.A., "Pyrolysis and Burning of Single Sticks of Pine in a Uniform Field of Temperature, Gas Composition, and Gas Velocity," *Combustion and Flame*, **46**, pp. 221-251, The Combustion Institute, 1982.
20. Becker, H.A., and Phillips, A.M., "Burning of Pine in Wind at 357-857 C and 3-18 m/s: The Wave Propagation Period," *Combustion and Flame*, **58**, pp. 273-289, The Combustion Institute, 1984.
21. Tse, S.D., and Fernandez-Pello, A.C., "On the Flight Paths of Metal Particles and Embers Generated by Power Lines in High Winds – A Potential Source of Wildland Fires," *Fire Safety Journal*, **30**:4, pp. 333-356, 1998.

Figures and Tables

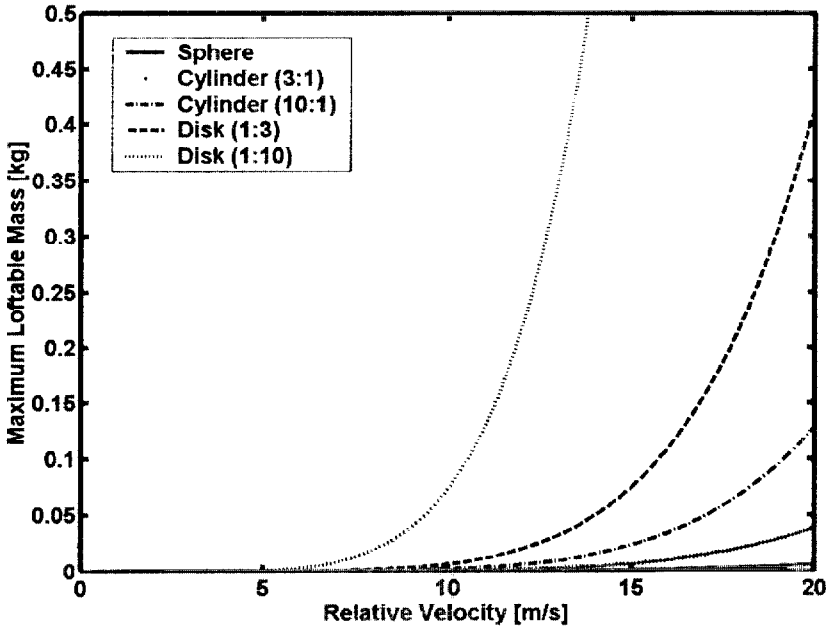

Figure 2: Maximum loftable mass for a given relative velocity as a function of brand shape for a diameter of 50 mm and length-to-diameter ratio as indicated.

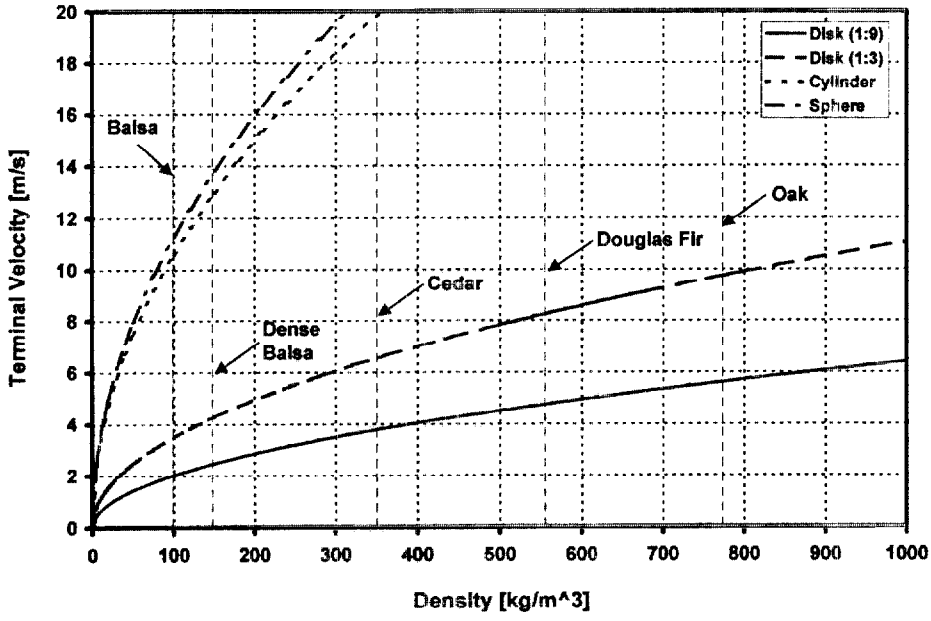

Figure 3: Terminal velocity for brands with a diameter of 50 mm and thickness-to-diameter ratio for disks as given; length does not affect terminal velocity for cylinders. Disk terminal velocity depends only on thickness for a given sample density. 25-mm-diameter disks have terminal velocities that are smaller by a factor of $\sqrt{2}$.

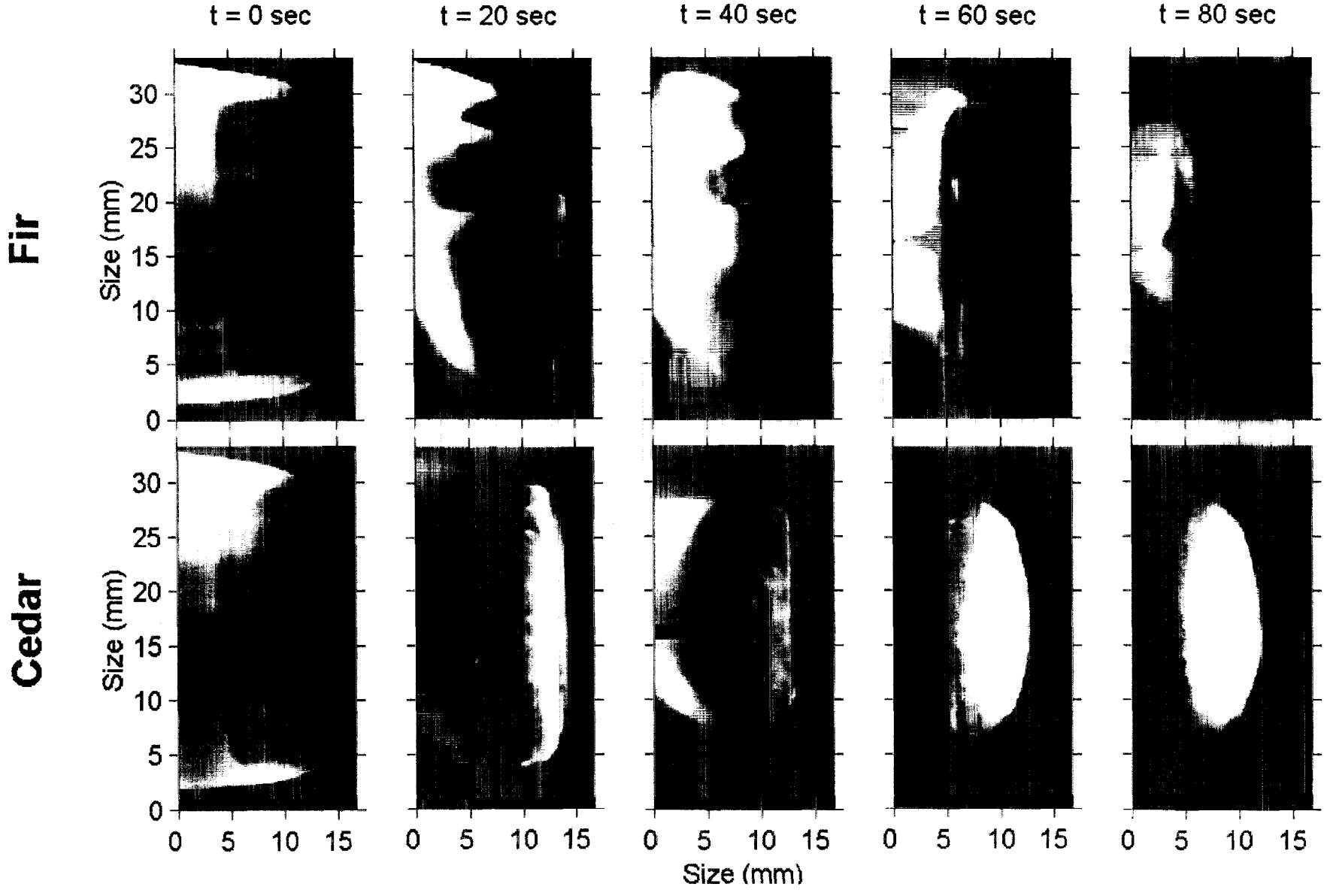

Figure 4: Comparison of combustion images for Douglas Fir and Western Red Cedar samples with a 1.8 m/s relative velocity. Both pieces were 25 mm in diameter and 8 mm thick. The fir extinguished at 90 s with 50% residual mass. The cedar burned to completion after 210 s.

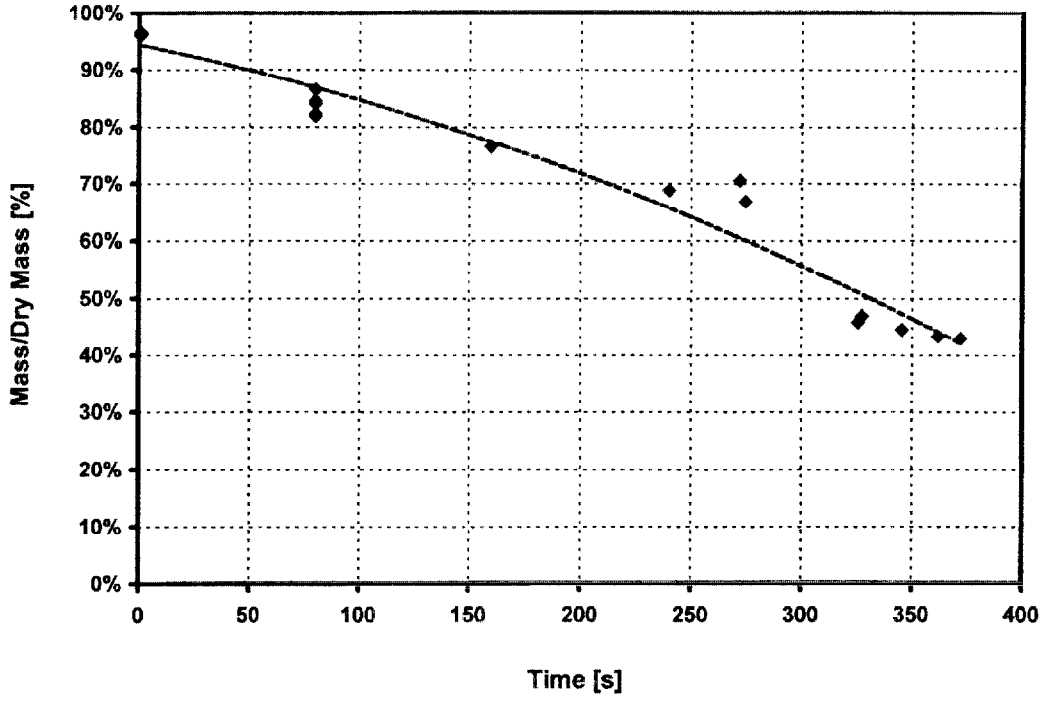

Figure 5: Mass history for 50mm diameter, 16 mm thick Douglas Fir disks. Experiments were terminated at 0, 80, 160, and 240 seconds by immersing the samples in CO_2. Data for times longer than 240 s represent samples that self-extinguished.

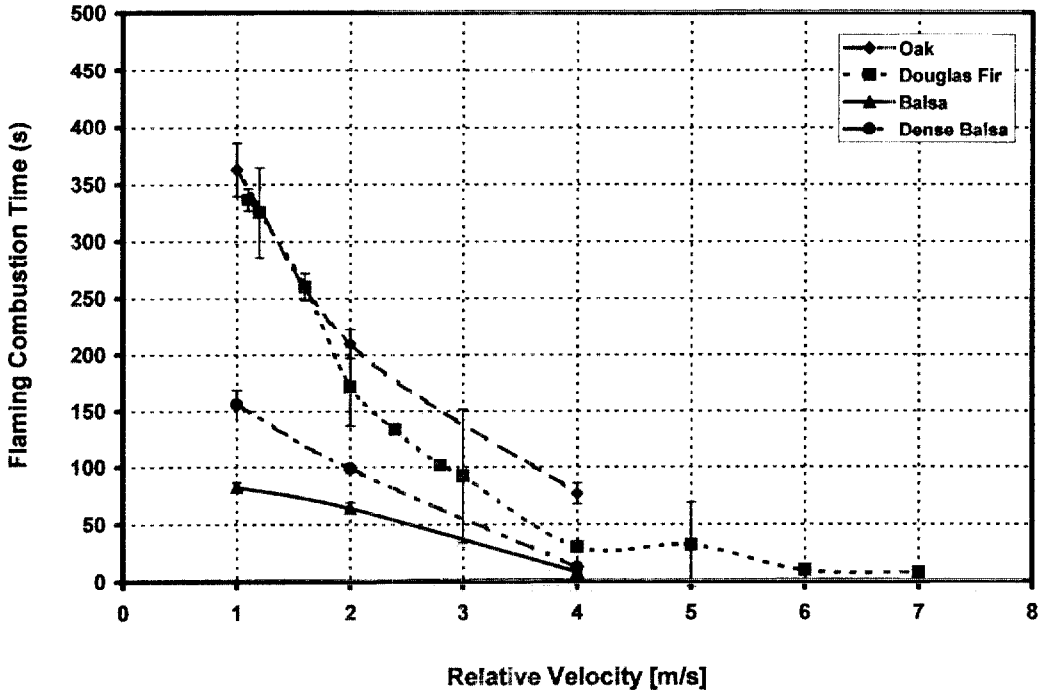

Figure 6: Time at which flaming combustion ceases as a function of relative velocity for a variety of wood types, where the initial diameter is 50mm and the thickness is 16mm.

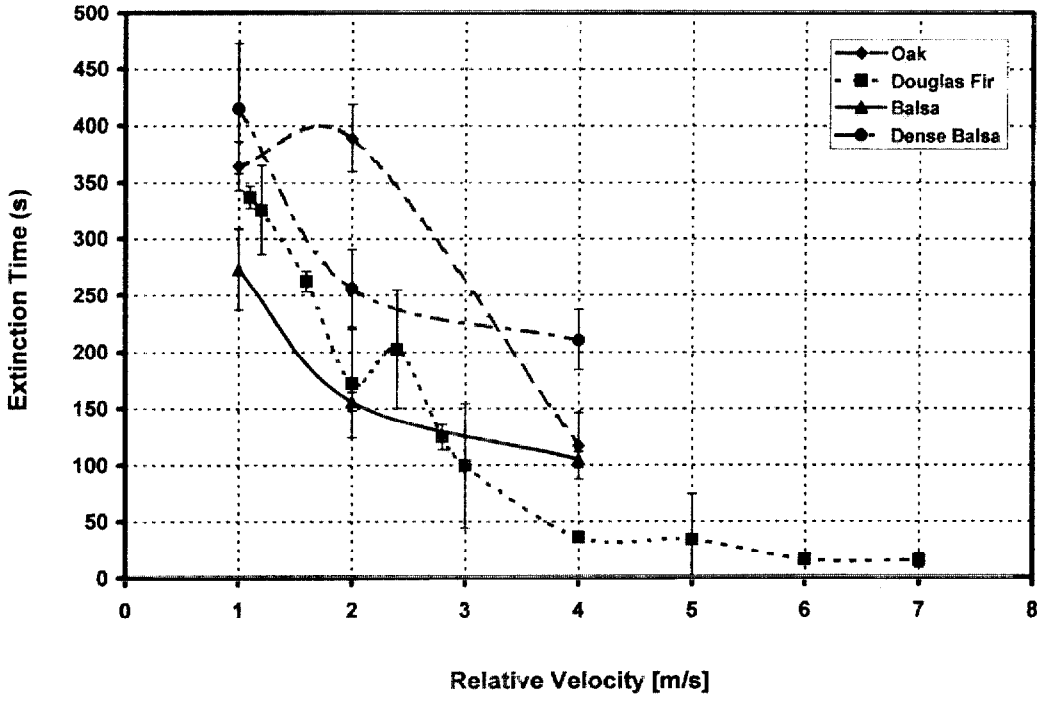

Figure 7: Average time at which brand self-extinguished as a function of relative velocity and wood type for disks 50 mm in diameter and 16 mm thick. Error bars denote standard deviation of 2 to 7 repetitions.

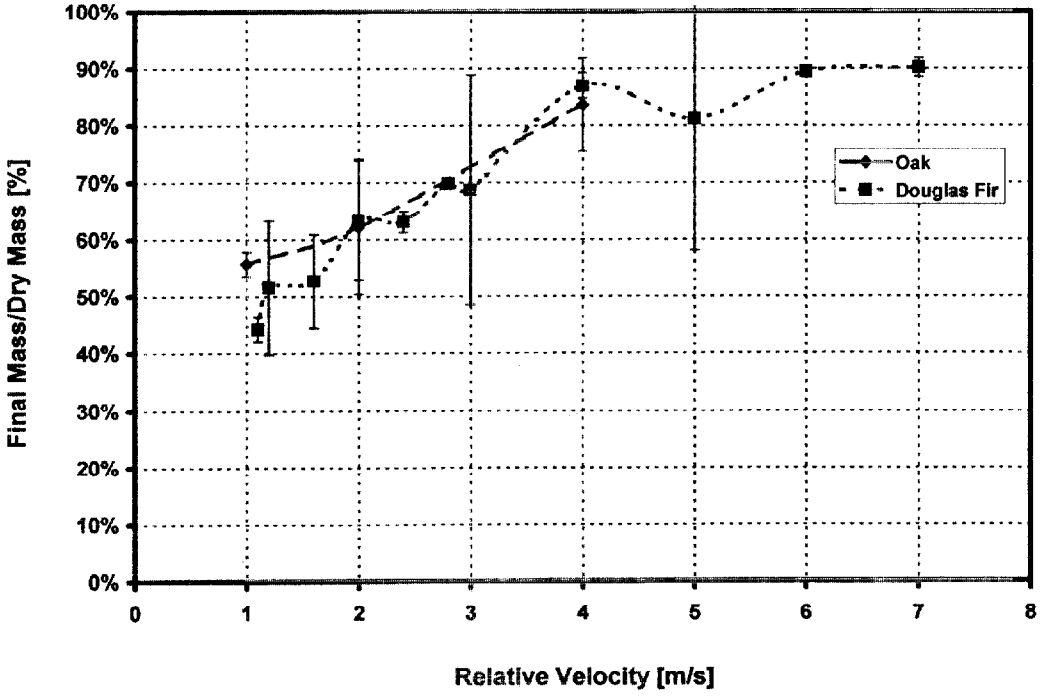

Figure 8: Percentage of dry mass at self-extinguishment as a function of relative velocity for Oak and Douglas Fir disks, 50 mm in diameter and 16 mm thick. Balsa samples burned to completion.